AJNR

Bilateral neonatal Sturge-Weber-Dimitri disease: CT and MR findings.

J W Yeakley, M Woodside and M J Fenstermacher

AJNR Am J Neuroradiol 1992, 13 (4) 1179-1182
http://www.ajnr.org/content/13/4/1179

Bilateral Neonatal Sturge-Weber-Dimitri Disease: CT and MR Findings

Joel W. Yeakley,[1,3] Marilyn Woodside,[2] and Marc J. Fenstermacher[1]

Summary: The CT and MR features of cortical calcification and meningeal angiomatosis are typical of Sturge-Weber-Dimitri disease but are unusual in children less than 1 year of age. This case describes a child presenting with both of these features bilaterally in the neonatal period and represents an unusual presentation of this disorder.

Index terms: Phakomatoses; Computed tomography, in infants and children; Magnetic resonance, in infants and children; Pediatric neuroradiology

We present a case of Sturge-Weber-Dimitri disease (SWDD) that demonstrates many unusual characteristics of this disease, including bilateral involvement, presentation in the neonatal period with cortical calcification already present, and angiomatosis demonstrable by CT and MR.

Case Presentation

A full-term girl with a midline facial nevus flammeus involving the forehead and nasal bridge was the product of an uncomplicated pregnancy and delivery. Physical examination showed a 2.5 × 6.5 cm nevus flammeus over the midline forehead and nasal bridge (Fig. 1). There were also small nevi involving the left upper and lower eyelids, the left temporal region, the nape of the neck, and left tibial region. The head circumference of 34 cm was at the 15th percentile, while her weight and height were 25th and 10th percentile, respectively. The newborn neurologic examination was within normal limits. Although there was no evidence of glaucoma initially, she subsequently developed glaucoma in the left eye, requiring trabeculectomy. An electroencephalogram on the third day of life was abnormal, with immaturity of background pattern and excessive sharp wave activity, especially during sleep. Titers for toxoplasmosis, rubella, and cytomegalic-inclusion disease were negative. Angiography was not performed. The patient developed clinical seizures at 5 weeks of age that were controlled with phenobarbital.

Computed tomography (CT) was performed without and with intravenous contrast, utilizing 5-mm sections. The noncontrast CT scans revealed an hourglass deformity of the brain with nonclosure of the sylvian fissures, as well as multifocal bilateral areas of atrophy with heavy calcification in the atrophic brain that followed a gyriform pattern (Fig. 2A). The calcification was not confined to the immediate subependymal periventricular region, but rather involved cortical areas. The lateral ventricles were mildly dilated. The contrast scan indicates that the space between the inner table of the skull and the brain, presumably representing subarachnoid space, is not purely cerebrospinal fluid density, but is occupied by numerous areas of serpiginous contrast enhancement compatible with vascular structures (Fig. 2B). The enhancing choroid plexus of the lateral ventricles is prominent bilaterally (Fig. 2C).

Magnetic resonance (MR) images were also obtained. The sagittal and coronal T1-weighted images show severe brain dysplasia with areas of cortical and subcortical high signal and widened "subarachnoid space" (Figs. 3A and 3B). The axial T2-weighted spin-echo and gradient-echo MR scans confirm the presence of low-signal areas corresponding to the calcifications seen on CT. There are generally gyriform, and in some areas assume the typical "tram-track" configuration expected of SWDD (Figs. 3C and 3D). The calcification is not confined to the periventricular subependymal region, as one would expect with TORCH, but affects areas primarily cortical and subcortical. In fact, the calcifications are located in the most atrophic or dysplastic areas that underlie multiple serpiginous low-signal areas thought to represent abnormal vasculature, as one might expect with SWDD angiomatous malformation. That the serpiginous structures represent vasculature is supported by the low-signal flow void within them, especially on the T2-weighted spin-echo and gradient-echo images where there is marked contrast between these structures and the surrounding high-signal cerebrospinal fluid (Figs. 3C and 3D). These appear to represent the same structures that enhanced with intravenous contrast on the CT scan. The gyral pattern appears abnormal, with a mulberry-like configuration in some areas suggesting polymicrogyria, whereas other areas seem smooth, resembling lissencephaly or pachygyria.

Received July 23, 1991; accepted and revision requested September 11; revision received September 30.

[1] Department of Radiology and the [2] Department of Neurology, The University of Texas Medical School at Houston, TX.

[3] Address reprint requests to Joel W. Yeakley, MD, Department of Radiology, The University of Texas Medical School at Houston, 6431 Fannin, 2.132 MSB, Houston, TX 77030.

AJNR 13:1179–1182, Jul/Aug 1992 0195-6108/92/1304-1179

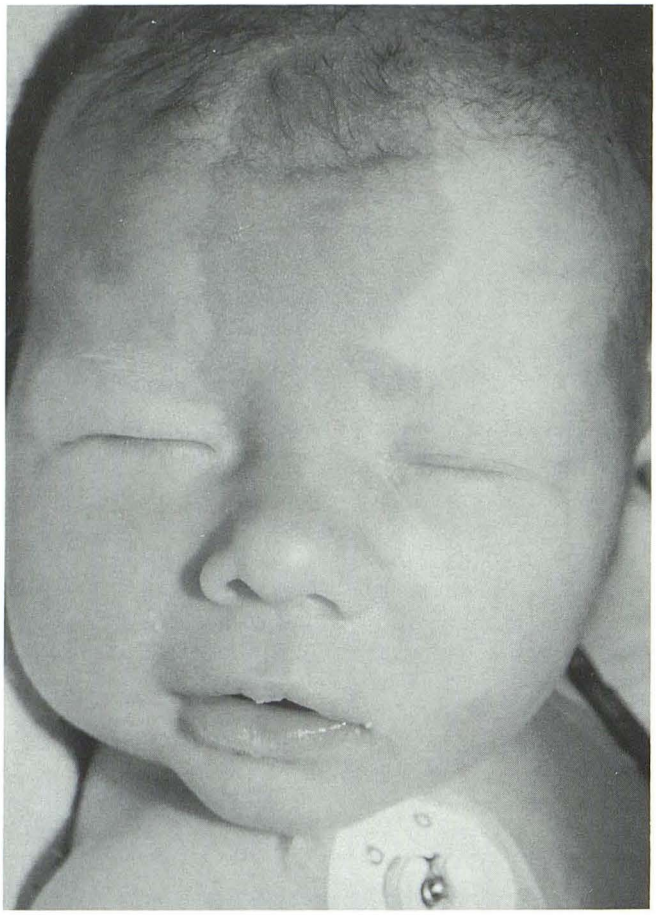

Fig. 1. Photograph of the patient's extensive nevus flammeus. Note that the bulk of the nevus flammeus is in the midline, which correlates with the bilateral intracranial abnormality.

Discussion

Encephalotrigeminal angiomatosis, or Sturge-Weber-Dimitri disease, is usually unilateral, although bilateral cases have been reported (1–3). Neonatal SWDD has also been reported (2, 4, 5). Other studies have commented on the relationship of the leptomeningeal angiomatosis to the development of cortical calcification (2, 6), and to associated venous abnormalities (5, 6). MR studies of SWDD have also been reported (7–9). However, we have not seen a case in the literature that brings together all of these components so dramatically.

It is generally reported that the calcification does not usually present at birth (10), but develops later as the leptomeningeal angiomatosis regresses (2, 6), frequently in conjunction with thrombosis of cortical veins or venous sinuses (6, 8). However, in this case, we see cortical calcification with identifiable abnormal vasculature presumably related to the venous component of angiomatosis (2). It has been unclear in the literature whether gyriform enhancement on CT or abnormal nuclear scintigram findings are related to the leptomeningeal angiomatosis itself, or related to abnormal permeability of cortical vessels with resultant cortical stain, or both (10, 11). In this case, we are able to define enhancement in the angiomatous vessels on CT rather than within the cortex itself. Enhancement of the angiomatous malformation on MR utilizing gadopentetate

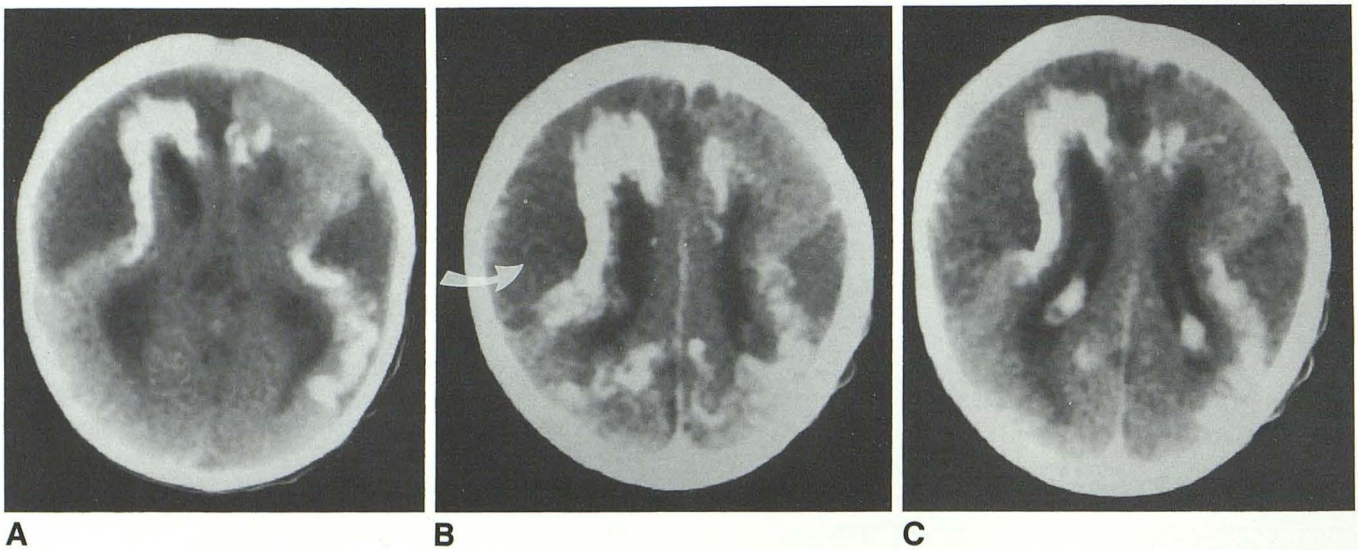

Fig. 2. *A*, CT scan without contrast shows somewhat hourglass shape of the brain with extensive cortical and subcortical calcification that appears gyriform in some areas. Note the poorly formed opercula and widened subarachnoid space in areas overlying the calcification.

B and *C*, Intravenous contrast administration reveals serpiginous areas of enhancement in the subarachnoid space overlying an area of abnormally calcified "atrophic" cortex (*arrow*) (*B*) and more prominent than usual choroid plexus enhancement (*C*).

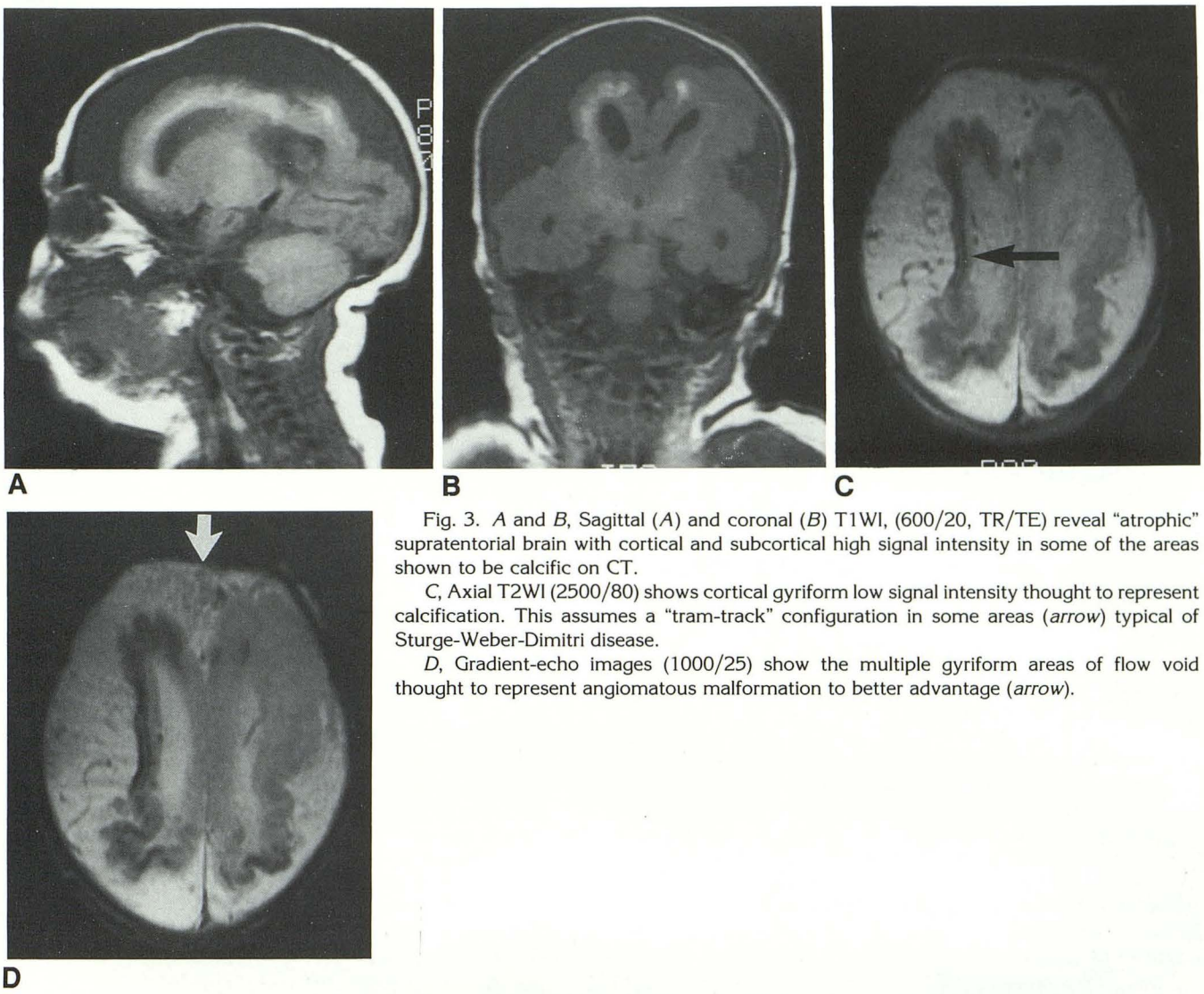

Fig. 3. *A* and *B*, Sagittal (*A*) and coronal (*B*) T1WI, (600/20, TR/TE) reveal "atrophic" supratentorial brain with cortical and subcortical high signal intensity in some of the areas shown to be calcific on CT.

C, Axial T2WI (2500/80) shows cortical gyriform low signal intensity thought to represent calcification. This assumes a "tram-track" configuration in some areas (*arrow*) typical of Sturge-Weber-Dimitri disease.

D, Gradient-echo images (1000/25) show the multiple gyriform areas of flow void thought to represent angiomatous malformation to better advantage (*arrow*).

dimeglamine or Gd-DOTA has recently been reported (12, 13). The angiomatous malformation of the choroid plexus in SWDD described by Stimac et al (14) is present bilaterally in this case.

Gyriform calcification has been reported in other conditions, especially the TORCH syndrome (15). However, in this case, the titers were negative and the calcifications do not fit the pattern of subependymal periventricular calcification usually seen with those conditions. Other reported conditions associated with gyriform calcification include celiac disease (16), ruptured dermoid with chemical meningitis (17), migraine-like headaches (18), leukemia after chemotherapy or radiation (10, 19), slowly growing oligodendroglioma (10) or other glioma (19), and purulent meningitis (15).

There are other features of this case that are atypical for SWDD, such as the extent of the facial angioma, which is more extensive than is typically seen. However, the bilateral presentation of the facial nevus correlates well with the bilateral intracranial findings. The type of calcification seen in some areas in this case is very dense and occupies almost the entire thickness of the cortex, which is unusual for SWDD. Alternatively, therefore, the dystrophic calcification could be related to cortical injury that occurred in utero. Yet there are areas in which the tram track appearance of typical of SWDD occurs. Extensive vascular occlusive disease, such as Moya Moya, may present early in life and may appear as extensive areas of dystrophic calcification in the cortex due to ischemia, but should not be associated with meningeal or venous angiomatosis such as we see in this case. Although migrational defects have rarely been found in SWDD, polymicrogyria, pachygyria, and lissencephaly have

been reported (2). In addition, Hooft et al (20) have described a rare form of meningeal angiomatosis associated with leukodystrophy that presented in infancy as diffuse sclerosis and cortical calcification associated with meningeal angiomatosis.

One possible explanation of the areas of increased signal on the T1-weighted MR images (Figs. 3A and 3B) might be the presence of calcium salts decreasing the T1 of surrounding water, as reported by Dell et al (21) and, more recently, by Henkelman et al (22). Neuropathologic findings in SWDD cases have demonstrated calcification in subcortical white matter as well as in cortical gray matter (23). Another possible explanation might be accelerated myelination reported by MR in early SWDD (8, 24).

This case presents many features consistent with Sturge/Weber/Dimitri disease in an usual combination that may suggest expanding the criteria for diagnosis.

References

1. DeMarco P, Lorenzin G. Growing bilateral occipital calcifications and epilepsy. *Brain Dev* 1990;12:342–344
2. Nellhaus G, Haberland C, Hill BJ. Sturge-Weber disease with bilateral intracranial calcifications at birth and unusual pathologic findings. *Acta Neurol Scand* 1967;43:314–347
3. Boltshauser E, Wilson J, Hoare RD. Sturge-Weber syndrome with bilateral intracranial calcification. *J Neurol Neurosurg Psychiatry* 1976;39:429–435
4. Welch K, Naheedy MH, Abroms IF, Strand RD. Computed tomography of Sturge-Weber syndrome in infants. *J Comput Assist Tomogr* 1980;4:33–36
5. Kitahara T, Maki Y. A case of Sturge-Weber disease with epilepsy and intracranial calcification at the neonatal period. *Eur Neurol* 1978; 17:8–12
6. Bentson JR, Wilson GH, Newton TH. Cerebral venous drainage pattern of the Sturge-Weber syndrome. *Radiology* 1971;101:111–118
7. Chamberlain MC, Press GA, Hesselink JR. MR imaging and CT in three cases of Sturge-Weber syndrome: prospective comparison. *AJNR* 1989;10:491–496
8. Jacoby CG, Yuh WTC, Afifi AK, Bell WE, Schelper RL, Sato Y. Accelerated myelination in early Sturge-Weber syndrome demonstrated by MR imaging. *J Comput Assist Tomogr* 1987;11:226–231
9. Wasenko JJ, Rosenbloom SA, Duchesneau PM, Lanzieri CF, Weinstein MA. The Sturge-Weber syndrome: comparison of MR and CT characteristics. *AJNR* 1990;11:131–134
10. Coulam CM, Brown LR, Reese DF. Sturge-Weber syndrome. *Semin Roentgenol* 1976;1:55–60
11. Kuhl DE, Bevilacqua JE, Mishkin MM, Sanders TP. The brain scan in Sturge-Weber syndrome. *Radiology* 1972;103:621–626
12. Lipski S, Brunelle F, Aicardi J, Hirsch JF, Lallemand D. Gd-DOTA-enhanced MR imaging in two cases of Sturge-Weber syndrome. *AJNR* 1990;11:690–692
13. Elster AD, Chen MY. MR imaging of Sturge-Weber syndrome: role of gadopentetate dimeglumine and gradient-echo techniques. *AJNR* 1990;11:684–689
14. Stimac GK, Solomon MA, Newton TH. CT and MR of angiomatous malformations of the choroid plexus in patients with Sturge-Weber disease. *AJNR* 1986;7:623–627
15. Ketonen L, Koskiniemi M. Gyriform calcification after herpes simplex virus encephalitis. *J Comput Assist Tomogr* 1983;7:1070–1072
16. Molteni N, Bardella MT, Baldassarri AR, Bianch PA. Celiac disease associated with epilepsy and intracranial calcifications: report of two patients. *Am J Gastroenterol* 1988;83:992–994
17. Machen BC, Williams JP, Lum GB, Joslyn JN, Silverboard G. Intracranial gyriform calcification associated with subarachnoid fat. *J Comput Assist Tomogr* 1986;10:385–388
18. Battyistella PA, Mattesi P, Casara GL, et al. Bilateral cerebral occipital calcifications and migraine-like headache. *Cephalalgia* 1987;7: 125–129
19. Borns PF, Rancier LF. Cerebral calcification in childhood leukemia mimicking Sturge-Weber syndrome. *AJR* 1974;122:52–55
20. Hooft C, Deloore G, Van Bogaert L, Guazzi GC. Sudanophilic leucodystrophy with meningeal angiomatosis in two brothers: infantile form of diffuse sclerosis with meningeal angiomatosis. *J Neurol Sci* 1965;2:30–51
21. Dell LA, Brown MS, Orrison WW, Eckel CG, Matwiyoff NA. Physiologic intracranial calcification with hyperintensity on MR imaging: case report and experimental model. *AJNR* 1988;9:1145–1148
22. Henkelman RM, Wahs JF, Kucharczyk W. High signal intensity in MR images of calcified brain tissue. *Radiology* 1991;179:199–206
23. Alexander GL, Norman RM. *The Sturge-Weber syndrome.* Bristol, England: John Wright, 1960
24. Crawford SC, Boyer RS, Harnsberger H, Pollei SR, Smoker WRK, Osborn AG. Disorders of histogenesis: the neurocutaneous syndromes. *Semin Ultrasound CT MR* 1988;3:247–267